

Structural And Functional Characterization Of Cation-Transporting Atpase Of Mycobacterium Tuberculosis CDC 1551 By In Silico Methods

C Kumar, C Anuradha, K Venkateswara Swamy, N Khan

Citation

C Kumar, C Anuradha, K Venkateswara Swamy, N Khan. *Structural And Functional Characterization Of Cation-Transporting Atpase Of Mycobacterium Tuberculosis CDC 1551 By In Silico Methods*. The Internet Journal of Genomics and Proteomics. 2005 Volume 2 Number 1.

Abstract

The three dimensional (3-D) structure of cation-transporting ATPase (ctATPase) of Mycobacterium tuberculosis CDC 1551 has been generated from amino acid sequence using homology modeling with backbone structure of calcium ATPase of *Oryctolagus cuniculus* as template. The model was generated using the method of satisfaction of spatial restraints by mod6v2 version of MODELLER. The generated 3-D structure of ctATPase) of *M. tuberculosis* was evaluated at various web interfaced servers i.e., WHAT IF, PRODOM, Pfam and PROCHECK which checks the stereo chemical quality of the structure in terms of bonds, bond angles, dihedral angles and non-bonded atom-atom distances, structural as well as functional domains etc., The generated model was visualized using the RASMOL visualization tool.

INTRODUCTION

With it's re-emergence, tuberculosis (TB) has become a major health problem worldwide and now a days it became a global emergency. It causes nearly 3 million deaths annually and an estimated 8.8 million new cases are reported every year. *M. tuberculosis* strain CDC 1551 is a highly transmissible strain which exhibited unusually high levels of infectivity and virulence during a recent outbreak of tuberculosis in a rural community. The complete genome of CDC 1551 (EMBL Accession number AE000516) consists of 4,403,836 base pairs [9,13]. This strain develops lung and spleen infections that are nearly identical to those caused by *Mycobacterium tuberculosis* strains Erdman, H37RV and Indian. Iron acquisition is critical for *M. tuberculosis* survival and replication in the infected host. Iron is essential as a cofactor of enzymes involved in vital cellular functions ranging from respiration to DNA replication. Limitation of this metal triggers an extensive response aimed at enhancing iron acquisition while coping with iron deficiency. Pathogens have to compete for iron in the host in order to multiply and establish a successful infection [16]. Studies in *M. tuberculosis* using one- and two-dimensional gel electrophoresis combined with mass spectroscopy and sequence information have shown that the levels of several proteins change in response to iron availability [22]. Among

these, a putative cation-transporting ATPase was induced in bacteria grown in a low-iron medium suggesting its importance in the maintenance of vital processes that depend on iron-containing cofactors including electron transport, energy metabolism and DNA synthesis [8]. The ctATPase plays a major role in the influx of ferrous ions during iron deficiency in the bacterium. They perform multiple vital functions in the cells which include ATPase activity coupled to trans-membrane movement of ions (ion-transport), phosphorylative mechanism, hydrolase activity and regulation of cation homeostasis [8]. Bacteria use ctATPase to pump out toxic heavy metal ions. These ATPases are important for intracellular bacteria like *M. tuberculosis*, which require transition metal cations for the synthesis of superoxide dismutases, and catalases which constitute an important line of defense against macrophage's killing mechanisms [10,16]. There is now compelling evidence that iron acquisition is critical for *M. tuberculosis* survival and replication in infected host. Hence present study has been conducted to understand and elucidate the 3-D structure of ctATPase of *M. tuberculosis* by homology modeling. Through the insights gained from its 3-D structure, the functionally important domains are well characterized. Knowledge of these structural features of ctATPase of *M. tuberculosis* is essential for establishing its catalytic action mechanism at molecular level as well to target the protein

for designing effective and selective drug.

METHODOLOGY

The ctATPase of *M. tuberculosis* CDC 1551 (gil158394831) having 752 amino acids was modeled by using ATPase *Oryctolagus cuniculus* as a reference template (PDB ID :1VFP) whose crystal structure is known at 2.6Å resolution (<http://www.rcsb.org/pdb>). Structural homologue to target sequence was found by BLAST-p against PDB database at <http://www.ncbi.nlm.nih.gov/BLAST> [1]. The 3-D structure of ctATPase of *M. tuberculosis* CDC 1551 was generated by homology modeling routine of MODELLER release 6v2. This routine includes the satisfaction of spatial and geometric restraints and a very fast molecular dynamic annealing; no other refinements were applied. MODELLER accepts the alignment of the sequence to be modelled with related known structures and automatically calculates a model with all non-hydrogen atoms that satisfies the restraints as well as possible and 3-D model was obtained by optimization of a molecular probability density function [2]. Thus generated 3-D structure was visualized by RASMOL [19]. The stereo chemical quality of the structure was analyzed using PROCHECK [15] which uses Ramchandran map [17] to check peptide bond planarity, bond lengths, bond angles, hydrogen bond geometry, and side chain conformations of protein structures as a function of atomic resolution. The functional domains of ctATPase of *M. tuberculosis* were obtained by submitting 3-D structure to Pfam at <http://www.sanger.ac.uk/Software/Pfam> [4, 5]. Prediction of secondary structure was done at WHAT IF (<http://swift.cmbi.kun.nl/whatif/>) [21]. The sequence segment domains for ctATPase were found in Swiss Prot database by BLASTp and the same were aligned by multiple sequence alignment using PRODOM at <http://prodes.toulouse.inra.fr/prodom.html> [7].

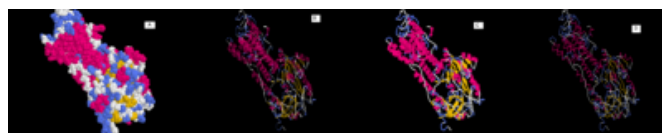
RESULTS

Most functional restraints on evolutionary divergence operate at the level of tertiary structure hence 3-D structures are more conserved in evolution than sequence [3]. The 3D structure of protein is an important source of information to better understand the function of a protein, its interactions with other compounds (ligands, proteins, DNA) and to understand phenotypical effects of mutations [20]. A large number of techniques have been developed to predict 3-D structures of proteins among which homology modeling is one of the best [14]. Homology modeling is historically the first [6] and MODELLER has been considered as most

accurate method [18]. Hence in the present study also we used homology modeling using MODELLER to generate the 3-D structure of ctATPase. The 3-D structure of ctATPase in *M. tuberculosis* CDC 1551 generated from MODELLER contains large bifurcated beta-sheets (mainly anti parallel) covered on both sides with helices and loops (Fig1 A-D). The ctATPase structure showed trans-membrane helices (Figure 1-C), some of which are well conserved throughout the super family thus they all operate via a similar mechanism. The beta sheet covered on both sides with helices and loops is probably the region where the ferric ion or other cations bind before being channeled down through the trans-membrane helices.

Figure 1

Figure 1: Cation transporting ATPase (ctATPase) of CDC 1551. Model generated MODELLER mod.6v2 version. The 3-D structure of ctATPase was visualized with RASMOL and represented in the form of spacefill (A), cartoons (B), ribbons (C) and backbone (D).



The predicted secondary structure of ctATPase obtained from WHAT IF server (Table 1) clearly indicated the sequence positions of different turns (79), helices (30) and sheets (28). Tentatively ctATPase structure was verified at PROCHECK (Table 2) and correspondingly Ramchandran plot (Figure 2) was also constructed to validate the structure [17].

Figure 2

Table 1: Secondary structure of ctATPase of CDC1551 obtained from WHAT IF (). The primary sequence of protein along with predicted secondary structures displayed simultaneously (H – helix, T – turns and S – sheets).

```

10 20 30 40 50 60
1- 60 MAAPVVGDDADLQSVRRIRLDVSGMSCAACASRVETKLNKIPGVRASVNFATRVATIDAVG
1- 60 TTTT TTT T TTTTTTTTT T HHHHHHHHHHHHHHHH TTTT
70 80 90 100 110 120
61- 120 MAADELCGWVEKAGYHAAPHTEITVLDIKRTKDPDGAHARRLLRLLVAALFVPLADLST
61- 120 HHHHHHT HHHHHHHHHHHHHHHHHHT SSSSTTTSSSSTTT TTT SSSSST
130 140 150 160 170 180
121- 180 LFAVPSARVPGVGYLTALAAPWTVAAWPFHVSVALRNARHRTTSMETLISVGIVAATA
121- 180 TSS TSSSSSS TT SSS TTTT TSS TTT TTSSSSS SSSSSST
190 200 210 220 230 240
181- 240 WSLSSVFGDQPPREGSGWRAILNDSIYLEVAAGVTVFVLAGRYFEARAKSKAGSALRA
181- 240 33THHHHHHTTT T TTHHHHHHHHHHHHHHHHHHHHHHHHHHHHHHTTT TTTT HHH
250 260 270 280 290 300
241- 300 LAELGAKNVAVLLPDGAELVPASELKIKRQRFVTRPGETIADGVVVDGSAIDMSAMTG
241- 300 HHHHHHHHHHHHT TTHHHHHHHHHHHHHHHHHHHHHHHHHHT SSSSTTHHHHHHHHH TSSSSST T
310 320 330 340 350 360
301- 360 EAKPVRAYPAASVVGVTVMVDGRLVIEATVAGDQTQFAAMVRLVEQAQTQKARQRLADH
301- 360 TT TT TTTTTT TTTT TT HHHHTTTT HHHHHH
370 380 390 400 410 420
361- 420 IAGVFPVVFVIAGLAGAAWLVSGAGADRAFVTLGVLVIACPCALGLATPTAMMVASGR
361- 420 TTTT TTT HHHH TT HHHHHHHHHHHHHHHHTTT SSSSST T
430 440 450 460 470 480
421- 480 GAQLGIFIKGYRALETIRSIDTVVFDKGTGLTVGQLAVSTVTMAGSGTSEDRDREVLGLA
421- 480 TT SSSSS TTHHHHHHHHHHTT SSSSS TT HHHHHHHHHHT S T
490 500 510 520 530 540
481- 540 AAVESASEHAMAAVAASPDPGPNVGFVAVAGCGVSGEVGGHHVEVGKPSWITRTPCH
481- 540 HHHHHHHH SS T TTT T TTT SSSSS TTHHHHHHHHTTSSS TTT HHHHH
550 560 570 580 590 600
541- 600 DAALVSARLDGESRGETVVFVSDGVVRAALTIADTLKDSAAAVALRSRGLRTILLTG
541- 600 TSSST THHHHHHHHHHHHHHHHHHHHHHHHHHHHHHHHHHTTTT HHHHHH
610 620
601- 624 DNRAAADAVAAQVGIDSAVADMLP
601- 624 HHHHHHTHHHHH333 TTT

625- 625 E
625- 625 ?
630 640 650 660 670 680
626- 685 GKVDVIQRLREEGHTVAMVGGDINDGPAALVADLGLAIGRGTVALGAADIILVRDDLNT
626- 685 HHHHHHHHHHTTTT TTT TTTT TTTT TTT THHHHHHHHHHH
690 700 710 720 730 740
686- 745 VPQALDLARATMRTIRMNMWAFGYNVAIPIAAAGLLNPLIAGAAMAFSSFFVVSNSLR
686- 745 3333TTTTTT TTTT 333 HHHHTTTTTHHHHHHHHTTTT TTTT TTTT TTTT
750
746- 752 LRNFGAG
746- 752 HHHHT
    
```

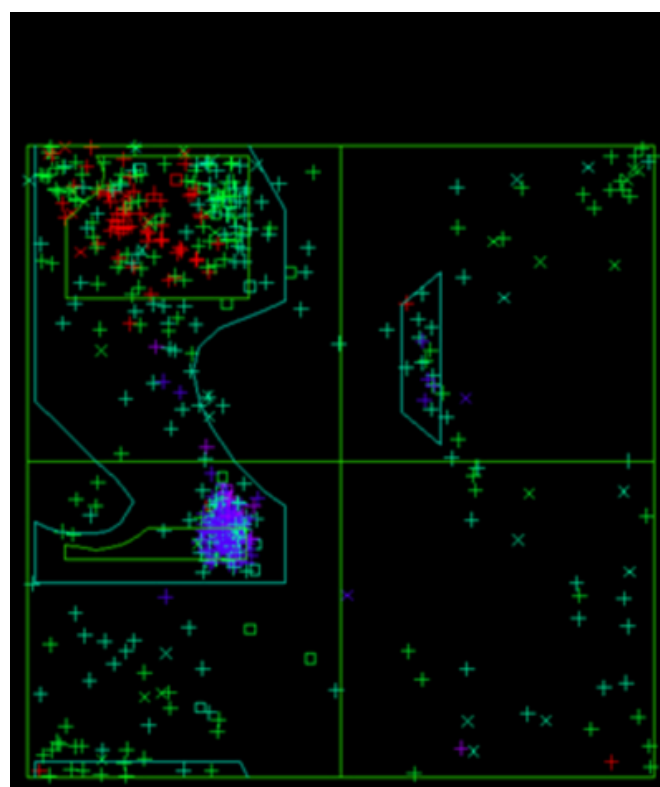
Figure 3

Table 2: Procheck summary for ctATPase of CDC1551 obtained at .

| PROCHECK SUMMARY | | | | |
|---------------------|---------------------------------|-------------------------|----------------|-------------|
| Test 2.0 | 752 residues | | | |
| Ramachandran plot | 76.0% core | 16.0% allow | 5.1% gener | 2.9% disall |
| Gly & Pro Ramach: | 7 labeled residues (out of 99) | | | |
| Chi1-chi2 plots: | 9 labeled residues (out of 332) | | | |
| Main-chain params: | 5 better | 0 inside | 1 worse | |
| Side-chain params: | 5 better | 0 inside | 0 worse | |
| Residue properties: | Bad contacts: 89 | | | |
| Bond len/angle: | 16.9 | Morris et al class: 1 1 | | 3 |
| G-factors | Dihedrals: - 39 | Covalent: -1.53 | Overall: -.81 | |
| M/c bond lengths: | 58.6% within limits | 41.4% highlighted | 21 off graph | |
| M/c bond angles: | 46.5% within limits | 53.5% highlighted | 41 off graph | |
| Planar groups: | 100.0% within limits | | 0% highlighted | |

Figure 4

Figure 2: Ramachandran Plot for generated 3-D structure of ctATPase of CDC 1551 obtained from WHAT IF web interface server. Color codes for secondary structures – blue -helix, red - strand and green - turns and random coil.



The function of a protein is generally determined by shape, dynamics and physiochemical properties of its solvent exposed molecular surface. Likewise functional differences

among the members of the same protein family are usually a consequence of the structural differences on the protein surface [11, 12]. Hence the functional domains of ctATPase were established through Pfam server and PRODOM and the results clearly revealed three major domains namely HMA (18-79 amino acids), E1-E2-ATPase (215-436 amino acids), and hydrolase (440-667 amino acids) which are responsible for heavy metal binding, phosphorylation activity and hydrolase activity of the protein respectively (Figure 3, Figure 4 and Table 3).

Figure 5

Figure 3: The ctATPase of showing three major domains. The HMA domain -green (18-79), E1-E2 ATPase domain - red (215-436) and Hydrolase domain - yellow (440-667). Results obtained from Pfam server and visualized with RASMOL(Ribbons)

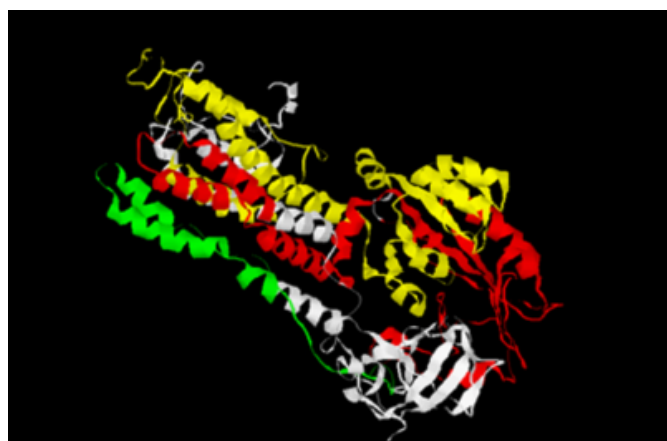


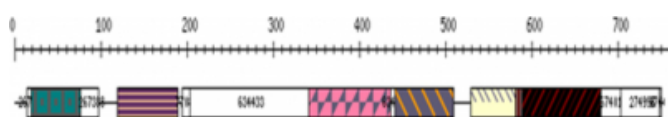
Figure 6

Table 3: Major functional domains of ctATPase of CDC1551. Domains, related bits score and e-values obtained from Pfam server which gives relationship of match sequences from server.

| Domain | Start | End | Bits | E-value |
|---------------------------------------|-------|-----|--------|---------|
| HMA | 18 | 79 | 59.90 | 7.2e-15 |
| E ₁ -E ₂ ATPase | 215 | 436 | 298.10 | 1.4e-86 |
| Hydrolase | 440 | 667 | 118 | 2e-32 |

Figure 7

Figure 4: Sequence segments from PRODOM for ctATPase of CDC1551 displaying with different color codes for different domain families. Obtained from PRODOM server at



DISCUSSION

Iron transport by ctATPase in *M. tuberculosis* is of great significance as iron is an essential nutrient whose concentration is critical in determining the outcome of infection with pathogenic CDC 1551 strain of *M. tuberculosis* and hence competition for iron plays a pivotal role in the interaction between host and parasite. Such clues can help in boosting up medical research to combat tuberculosis. Iron is an obligate cofactor for at least 40 different enzymes encoded in the *Mycobacterium tuberculosis* genome [8]. Cytochromes involved in electron transport, ribonucleotide reductases for DNA synthesis and superoxide dismutase for defense against macrophages are the three important enzymes that require iron [2]. Restricting access of this organism to iron can be adopted as an effective strategy for the treatment of the disease caused by it. *M. tuberculosis* CDC 1551 has evolved a complex web of biosynthetic and metabolic pathways to obtain, store and regulate the use of iron. Unraveling of the intricacies of this system may help in the development of new drugs for effective regulation of tuberculosis. Further progress towards new therapies to counter mycobacterial infection requires an even greater understanding of the complexities of proteins that interact with iron within the bacterium. Hence it is predicted that characterization of proteins involved in cation transport specifically ctATPase will provide complete understanding of *M. tuberculosis* iron acquisition machinery. This knowledge should provide new targets for therapeutic intervention against tuberculosis. The 3-D structure generated for ctATPase of *M. tuberculosis* CDC-1551 is further under investigation in our lab to establish its interaction with small inhibitor molecules (SIM) from ligand database using AUTODOCK and TRIPHOS software, which will result in emerging with new drugs to combat tuberculosis more effectively.

ACKNOWLEDGEMENTS

Authors are grateful to Prof. A. Sali, California Institute for Quantitative Biomedical Research, University of California, San Francisco, for permission to use MODELLER6V2. SKC thanks to UGC-New Delhi for financial support to establish computer networking Lab.

References

1. Altschul S.F., Grish W., Miller W., Myers E. W. and Lipman, D. J. (1990). Basic local alignment search tool. *J. Mol.Biol.* 215, 403-410.
2. Andrews, S. C.(1998). Iron storage in bacteria. *Adv. Microb. Physiol.* 40, 281-351.

3. Bajaj, M and Blundell, T. (1984). Evolution and the tertiary structure of proteins. *Ann. Rev. Biophys. Bioeng.* 13, 453-492.
4. Bateman A., Birney, E., Durbin, R., Eddy, S. R., Howe K L and Sonnhammer, E.L. (2000). The Pfam protein families database. *Nucleic Acids Res.* 28, 263-266.
5. Bateman A., Coin, L., Durbin, R., Finn, R.D., Hollich, V., Griffith Jones, S., Khanna, A., Marshal, M., Moxin, S., and Sonnhammer, E.L. (2004). The Pfam protein families database. *Nucleic Acids Res.* 32, D138-D141.
6. Browne, W.J., North, A.C. and Philips, D.C. (1996). A possible three dimensional structure of bovine alpha-lactalbumin based on that of hen's egg-white lysozyme. *J.Mol.Biool.*42, 65-86.
7. Bru , C., Coudrcelle, E., Carrere, S., Beause, Y., Dalmar, S and Kahn Daniel. (2005). The ProDom database of protein domain families: more emphasis on 3D. *Nucleic Acids Res.* 33, D212-D215.
8. Calder, K.M., and Horwitz, M.A. (1998). Identification of iron-regulated proteins of Mycobacterium tuberculosis and cloning of tandem genes encoding a low iron-induced protein and metal transporting ATPase with similarities to two-component metal transport systems. *Microb. Pathog* 24, 133-143.
9. Cole S.T., Brosch R., Parkhill J., Garnier T., Churcher C., Harris D., Gordon S.V., Eiglmeier K., Gas S., Barry C.E 3rd., Tekaiia F., Badcock K., Basham D., Brown D., Chillingworth T., Connor R, Davies R, Devlin K, Feltwell T, Gentles S, Hamlin N, Holroyd S, Hornsby T, Jagels K., Krogh A., McLean J., Moule S., Murphy L., Oliver K., Osborne J., Quail M.A., Rajandream M.A., Rogers J., Rutter S., Seeger K., Skelton J., Squares R., Squares S., Sulston J.E., Taylor K., Whitehead S. and Barrell B.G. (1998) Deciphering the biology of Mycobacterium tuberculosis from the complete genome sequence. *Nature (London)* 393, 537-544.
10. Dubnau, E., Fontan, P., Manganelli, R., Soares-Appel, S., and Smith, I. (2002) Mycobacterium tuberculosis genes induced during infection of human macrophages. *Infect Immun.* 70,2787-2795.
11. Fiser. A. and Sali. A. (2003). MODELLER: Generation and Refinement of Homology-Based Protein Structure Models. *Methods Enzymol.* 374,461-491.
12. Fiser. A., Do, R.K. and Sali. A. (2000). Modeling of loops in protein structure. *Protein Sci.*, 9, 1753-1773.
13. Fleischmann R.D., Alland D., Eisen J.A., Carpenter L., White O., Peterson J., DeBoy R., Dodson R., Gwinn. M., Haft. D, Hickey E, Kolonay J.F., Nelson W.C., Umayam L.A., Ermolaeva M., Salzberg .S.L., Delcher. A, Utterback. T., Weidman. J., Khouri. H., Gill. J., Mikula. A., Bishai. W., Jacobs. Jr. W.R Jr, Venter. J.C. and Fraser C.M. (2002). Whole genome comparison of Mycobacterium tuberculosis clinical and laboratory strains. *J Bacteriol.* 184(19), 5479-90.
14. Lambert. C., Leonard.N., De Bolle. X. and Depiereux. E. (2002). ESYPred3D: Prediction of proteins 3D structures. *Bioinformatics*, 18, 1250-1256.
15. Laskowski, R.A., MacArthur, M.W., Moss, D.S. & Thornton, J.M., (1993). PROCHECK: a program to check the stereo chemical quality of protein structures. *J. Appl. Crystallogr.* 26, 283-291.
16. Marcela Rodriguez G. and Issar Smith.(2003) Mechanism of iron regulation in Mycobacteria: role in physiology and virulence.*J. Mol.Micro.* 47(6),1485-1494.
17. Ramachandran G.N. and Sasisekharan, V. (1968). Conformation of polypeptides and proteins. *Adv Protein Chem.* 23, 283-438.
18. Sanchez, R and Sali, A. (1997) Advances in comparative protein structure modeling. *Curr. Opin. Struct. Biol.*,7, 206-214.
19. Sayle. R.A. and Milner White. E.J. (1995). RASMOL: bimolecular graphics for all. *Trends Biochem. Sci.* 20, 374.
20. Tramontano, A. (1998). Homology modeling with low sequence identity. *Methods*:14, 293-300.
21. Vriend G. (1999). WHAT IF: a molecular modeling and drug design program. *J. Mol. Graph.* 8, 52-56.
22. Wong. D., Lee, B.Y., Horwitz, M.A. and Gibson, B. (1999). Identification of Fur, aconitase and other proteins expressed by Mycobacterium tuberculosis under conditions of low and high concentrations of iron by combined two-dimensional gel electrophoresis and mass spectrometry. *Infect Immun.* 67, 327-336.

Author Information

Chitta Suresh Kumar, Ph.D.

Bioinformatics Center, Department of Biochemistry, Sri Krishnadevaraya University

C. M. Anuradha, M.Sc., M.Phil.

Bioinformatics Center, Department of Biochemistry, Sri Krishnadevaraya University

K. Venkateswara Swamy, M.Sc.

Bioinformatics Center, Department of Biochemistry, Sri Krishnadevaraya University

Niamat Ali Khan, M.Sc.

Bioinformatics Center, Department of Biochemistry, Sri Krishnadevaraya University